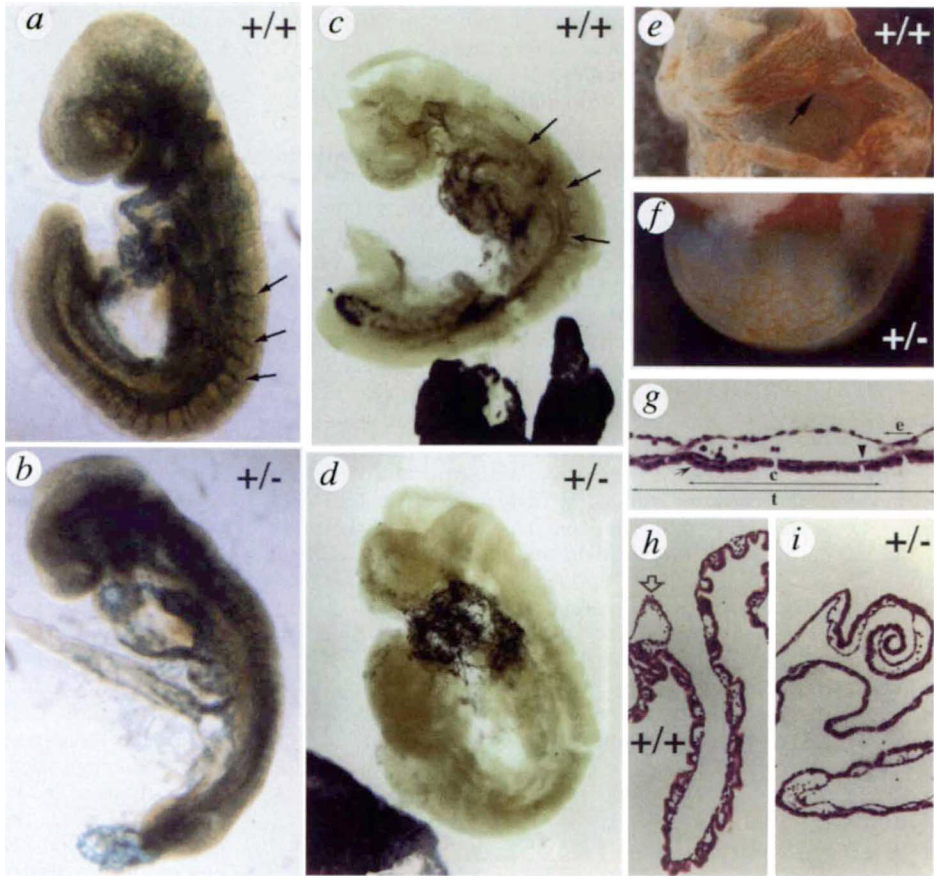

FIG. 3 *a*, *b*, Whole-mount LacZ staining revealing a dense network of sprouting vessels in the head mesenchyme and between the somites (arrows indicate intersomitic vessels), and the proper connections between the dorsal aortae and the heart of a 9.5-d.p.c. F_1 *VEGF*$^{+/+}$:*tie-1-lacZ*$^{+/-}$ *embryo (a)*. The 9.5-d.p.c. F_1 *VEGF*$^{+/-}$:*tie-1-lacZ*$^{+/-}$ *embryo (b)* contained a dorsal aorta that appeared as a vascular string with a reduced diameter, fewer intersomitic vessels, and abnormal organization of vessels, connecting with the heart. *c*, *d*, Injection of ink made visible the heart and the major intra-embryonic vessels (including the dorsal aorta; arrows in *c*) in the *riVEGF*$^{+/+}$, but only the heart in the *VEGF*$^{+/-}$ T-ES cell-derived embryo (both at 9.5-d.p.c.). *e*, *f*, Macroscopic examination of the yolk sac revealing the presence of a dense capillary plexus with larger collecting vessels (indicated by arrow) in the 9.5-d.p.c. F_1 *VEGF*$^{+/+}$ *yolk sac (e)*, but only an irregular and less dense network of wider capillaries without larger collecting vessels in the 9.5-d.p.c. F_1 *VEGF*$^{+/-}$ yolk sac (*f*). *g*, Section through a yolk sac, revealing an individual yolk-sac vessel with endothelial cells (arrowhead), and the visceral endoderm layer (arrow). Lines denote the cross-sectional length of the yolk-sac vessel, adjacent and parallel to the endoderm layer (c), the empty space between vessels (e) and the total yolk-sac length analysed (t). Measurements of these distances were used to calculate the vessel density (see Table 1*b*). *h*, *i*, Sections through a 9.5-d.p.c. F_1-*VEGF*$^{+/+}$ yolk sac (*h*), revealing a network of small vessels and a larger collecting vessel (open arrow), that connects with the intra-embryonic vitelline vessel. Sections through a 9.5-d.p.c. F_1-*VEGF*$^{+/-}$ yolk sac (*i*) revealed fewer but enlarged small yolk-sac vessels, and the absence of the larger collecting vessels.

METHODS. T-ES-derived embryos were dissected at 9.5-d.p.c. and filtered ink was immediately injected into the beating heart, using a heat-drawn capillary and a Narashigi micro-syringe-based injector. Dissection, fixation and staining of the embryos were done as described in Fig. 2.

5. Ferrara, N. *Trends cardiovasc. Med.* **3,** 244–250 (1993).
6. Shibuya, M. *et al. Oncogene* **5,** 519–524 (1990).
7. Devries, C. *et al. Science* **255,** 989–991 (1992).
8. Millauer, B. *et al. Cell* **72,** 835–846 (1993).
9. Mustonen, T. & Alitalo, K. *J. Cell Biol.* **129,** 895–898 (1995).
10. Breier, G., Albrecht, U., Sterrer, S. & Risau, W. *Development* **114,** 521–532 (1992).
11. Breier, G., Clauss, M. & Risau, W. *Devl. Dynam.* **204,** 228–239 (1995).
12. Shalaby, F. *et al. Nature* **376,** 62–66 (1995).
13. Fong, G.-H., Rossant, J., Gertsenstein, M. & Breitman, M. L. *Nature* **376,** 66–70 (1995).
14. Maglione, D., Guerriero, V., Viglietto, G., Delli-Bovi, P. & Persico, M. G. *Proc. natn. Acad. Sci. U.S.A.* **88,** 9276–9271 (1991).
15. Park, J. E., Chen, H. H., Winer, J., Houck, K. A. & Ferrara, N. *J. biol. Chem.* **269,** 25646–25654 (1994).
16. Nagy, A., Rossant, J., Nagy, R., Abramow-Newerly, W. & Roder, J. C. *Proc. natn. Acad. Sci. U.S.A.* **90,** 8424–8428 (1993).
17. Nagy, A. & Rossant, J. in *Gene targeting. A Practical Approach* (ed. Joyner, A. L.) 147–180 (IRL, Oxford, 1994).
18. Tischer, E. *et al. J. biol. Chem.* **266,** 11947–11954 (1991).
19. Claffey, K. P., Senger, D. R. & Spiegelman, B. M. *Biochim. biophys. Acta* **1246,** 1–9 (1995).
20. Pötgen, A. J. G. *et al. J. biol. Chem.* **269,** 32879–32885 (1994).
21. Friedrich, G. & Soriano, P. *Genes Dev.* **5,** 1513–1523 (1991).
22. Puri, M., Rossant, J., Alitalo, K., Bernstein, A. & Partanen, J. *EMBO J.* **14,** 5884–5891 (1995).
23. Risau, W. & Flamme, I. *A. Rev. Cell. Dev. Biol.* **11,** 73–92 (1995).
24. Alon, T. *et al. Nature Med.* **1,** 1024–1028 (1995).
25. Tybulewicz, V. *et al. Cell* **65,** 1153–1163 (1991).
26. Carmeliet, P. *et al. J. clin. Invest.* **92,** 2746–2755 (1993).
27. Risau, W. *et al. Development* **102,** 471–478 (1988).
28. Stavri, G. T. *et al. FEBS Lett.* **358,** 311–315 (1995).

SUPPLEMENTARY INFORMATION. Available at *Nature*'s World-Wide Web site http://www.nature.con; requests may also be addressed to Mary Sheehan at the London editorial office of *Nature*.

ACKNOWLEDGEMENTS. We thank K. Alitalo, A. Bernstein, J. Partanen, M. Puri and J. Rossant for the *tie-1-lacZ* transgenic mice; A. Damert for sequence information of the murine VEGF genomic clone; J. Herz for the JH_1 ES cells; and M. Baes, G. Carmeliet, M. Clauss, E. Conway, C. Lobe, M. Minne, J. Rossant and M. Sass and the other members of the CTTGT for help and discussions.

CORRESPONDENCE and requests for materials should be addressed to D. C. (e-mail: desire.collen@med.kuleuven.ac.be).

Heterozygous embryonic lethality induced by targeted inactivation of the VEGF gene

Napoleone Ferrara, Karen Carver-Moore, Helen Chen, Mary Dowd, Lucy Lu, K. Sue O'Shea*, Lyn Powell-Braxton, Kenneth J. Hillan & Mark W. Moore

Departments of Cardiovascular Research, Molecular Biology and Bioanalytical Technology, Genentech Inc., 460 Point San Bruno Boulevard, South San Francisco, California 94080, USA
* Department of Anatomy and Cell Biology, University of Michigan, Ann Arbor, Michigan 48109, USA

ANGIOGENESIS is required for a wide variety of physiological and pathological processes[1]. The endothelial cell-specific mitogen vascular endothelial growth factor (VEGF)[2,3] is a major mediator of pathological angiogenesis[4–6]. Also, the expression of VEGF and its two receptors, Flt-1 and Flk-1/KDR, is related to the formation of blood vessels in mouse and rat embryos[7–10]. Mice homozygous for mutations that inactivate either receptor die *in utero* between days 8.5 and 9.5 (refs 11,12). However, ligand(s) other than VEGF might activate such receptors[13,14]. To assess the role of VEGF

directly, we disrupted the VEGF gene in embryonic stem cells. Here we report the unexpected finding that loss of a single VEGF allele is lethal in the mouse embryo between days 11 and 12. Angiogenesis and blood-island formation were impaired, resulting in several developmental anomalies. Furthermore, VEGF-null embryonic stem cells exhibit a dramatically reduced ability to form tumours in nude mice.

We constructed a targeting vector in which the coding sequence of exon 3 of the VEGF[15] gene was replaced by a neomycin-resistance[16] (*neo*^{r}) gene (Fig. 1*a*). Two independent embryonic stem (ES) cell clones with a single VEGF allele mutation were identified (Fig. 1*b*), one of which was used to generate *VEGF*$^{-/-}$ ES cells (Fig. 1*c*). To confirm inactivation of the VEGF gene, we analysed the production of VEGF in ES cells by a radioreceptor assay[13], using the two VEGF receptors Flt-1 and Flk-1/KDR. ES cells subjected to a similar selection procedure to inactivate both alleles of the c-*mpl* gene, which encodes the thrombopoietin receptor[17], were included as controls. Wild-type and c-*mpl*$^{-/-}$ ES cells secrete similar amounts of activity able to compete with both receptors ($\sim$ 15 ng ml^{-1} after 48 h in culture); *VEGF*$^{+/-}$ cells secreted approximately half of that amount, whereas *VEGF*$^{-/-}$ cells released no VEGF. These findings confirm VEGF inactivation at the protein level and also argue against the possibility that the targeted protein may exert a dominant-negative effect on VEGF release in *VEGF*$^{+/-}$ cells.

We tested the hypothesis that VEGF mediates vasculogenesis *in vitro* by inducing embryoid body formation[18] in wild-type or *VEGF*$^{-/-}$ ES cells. Immunostaining with an antibody specific for CD34 revealed a vascular-like pattern in wild-type embryoid bodies, in agreement with previous studies[18], whereas embryoid bodies derived from *VEGF*$^{-/-}$ ES cells failed to develop any organized CD34-positive vessel-like pattern (unpublished observations).

We then used the nude mouse model to determine the role of VEGF in ES cell angiogenesis *in vivo* and in tumorigenesis[19]. Wild-type or c-*mpl*$^{-/-}$ ES cells formed rapidly growing tumours, whereas *VEGF*$^{-/-}$ ES cells had dramatically impaired ability to grow *in vivo*. The difference in tumour weight between c-*mpl*$^{-/-}$ and *VEGF*$^{-/-}$ clones was more than tenfold by four weeks after injection (Fig. 2*a*). Histologically, all of the ES-cell-derived tumours were germ-cell tumours containing a variety of differentiated and undifferentiated tissues, consistent with a teratoma[20]. Although blood vessels were identified in all groups, the number of vessels in the *VEGF*$^{-/-}$ group was strikingly reduced and showed a much less complex branching pattern than that observed in groups with at least one intact VEGF allele (Fig. 2*b–e*).

VEGF$^{+/-}$ ES cells were used to generate chimaeric mice[21,22], and both independent clones used transmitted the ES genetic information to the germ line, as assessed by agouti offspring. However, no viable heterozygous mice were obtained after $>$ 100 offspring, suggesting either that the loss of VEGF was lethal in the heterozygous state or that VEGF is maternally imprinted, which would effectively eliminate expression as the ES cells used are male. In blastocysts collected from females bred to germline-producing males, the mutant allele was detected by the polymerase chain reaction (PCR) at a mendelian ratio, confirming that faulty chromosomal transmission or loss in the ES cells was not responsible for the lack of heterozygous births. Presuming embryonic lethality, we collected embryos derived from germline-producing males at days E9.5–12.5. We observed a defect in blood supply of the yolk sac in several embryos at E9.5–11.5 (Fig. 3*a*). PCR analysis of these yolk sacs indicated that all aberrant embryos were positive for the *neo*^{r} gene, and that all normal embryos were wild-type. The *VEGF*$^{+/-}$ embryos exhibited several anomalies[23] (Fig. 3). In the cranial region, the branchial arches were poorly developed and unsegmented. The forelimb buds were positioned at their earlier caudal location and were unsegmented. Also, the forebrain region appeared significantly underdeveloped (Fig. 3*b*, *g*). In the heart region, the common atrium and primitive ventricle were developmentally delayed[23], the dorsal aortae were rudimentary, and the thickness of the ventricular wall was markedly decreased (Fig. 3*b*, *c*, *g*, *h*). Unlike the wild-type, in the mutant

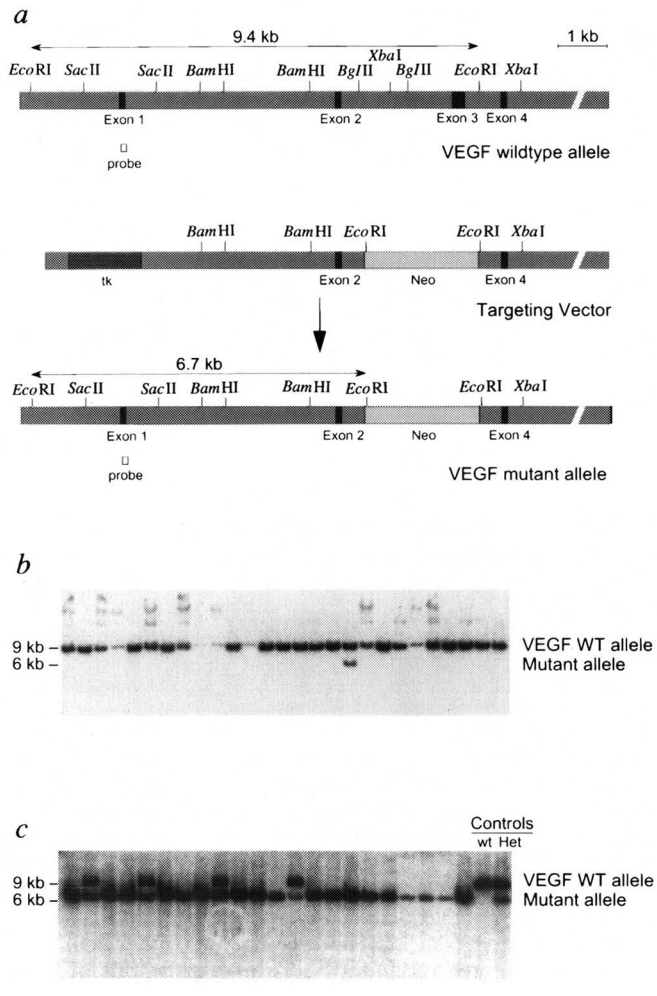

FIG. 1 Targeting vector (*a*) and Southern blot analysis of single (*b*) and double (c) allele targeted ES cells.

METHODS. An 18-kb genomic clone encompassing the 5′ end of the murine VEGF locus was isolated from a 129 λ FIX library (Stratagene) and characterized according to standard mapping procedures[27]. A 4.4-kb *Sac*II–*Bgl*II fragment encoding exon 2 and a 7.5-kb *Eco*RI–*Xho*I (vector) fragment containing exon 4 were ligated on either side of a *PGK–neo* cassette[16], thus deleting exon 3 (ref. 15). The *Bgl*II site was destroyed in the ligation and an *Eco*RI site was introduced in its place. The direction of transcription of the neomycin-resistance gene was in the opposite orientation to the VEGF gene. A CMV–TKpA cassette was added to the 5′ end of the construct to allow negative selection for homologous recombination[28]. Insertion of the *neo* cassette resulted in the creation of a new *Eco*RI fragment of 6.7 kb in contrast to the 9.4-kb wild-type allele. The targeting vector (20 μg) was linearized and electroporated at 275 V, 200 mF using a BTX 300 electroporator into a subclone of D3 ES cells (ES D3 C12). Cells were subjected to G418 selection[16] at 400 μg ml^{-1} and 0.2 μM 2-deoxy 2-fluoro-β-D arabinosyl-5-idouracil (FIAU) for 10 days. Single colonies were expanded for DNA isolation and Southern blot analysis using a 100-bp oligonucleotide probe homologous to exon 1 sequences which are not present in the targeting construct. The targeting frequency was 2 of 1,169 clones screened. The two clones were selected to generate chimaeric mice by microinjection into the blastocoele cavity of 3.5-day C57BL/6J blastocysts[21,22]. Chimaeric males were mated with C57BL/6J females and agouti offspring were screened for germline transmission by PCR analysis for the *neo*^{r} gene. No heterozygous mice were obtained. To generate *VEGF*$^{-/-}$ ES cells, a *VEGF*$^{+/-}$ clone was grown in 1.5 mg ml^{-1} G418 to select for cells that had two copies of the *neo*^{r} gene[29]. After 10–12 days, individual clones were expanded for DNA isolation and Southern analysis.

embryo the vitelline veins failed to fuse with the yolk sac (data not shown). The yolk sac revealed a substantially reduced number of nucleated red blood cells within the blood islands (Fig. 3*d*, *i*). This finding is consistent with there being insufficient activation of the Flk-1/KDR tyrosine kinase by VEGF[12]. Haematoxylin and eosin and CD34 immunostaining, revealed significant defects in the vasculature of other tissues and organs including placenta (Fig. 3*e*, *j*) and the nervous system. The vascular pattern of the forebrain in E10.5 wild-type and heterozygous embryos is shown in Fig. 4*a*, *b*, *e*, *f*. In the wild-type embryos, both the neuroepithelium and the adjacent mesenchyme contain numerous CD34-positive vessels (Fig. 4*a*, *b*), whereas vascular elements in heterozygotes could be demonstrated in the mesenchyme but not in the neuroepithelium (Fig. 4*e*, *f*). This failure of blood-vessel ingrowth was accompanied by apoptosis and disorganization of neuroepithelial cells (Fig. 4*e*, *f*). Consistent with the vascular deficit, apoptosis was dramatically increased in the mutant embryos at E11.5 (data not shown), and death occurs between days 11 and 12. Thus the *VEGF*$^{+/-}$ embryos survive approximately two days longer than the Flt-1 (ref. 11) or Flk-1/KDR (ref. 12) null embryos, presumably reflecting a partial activation of these tyrosine kinases.

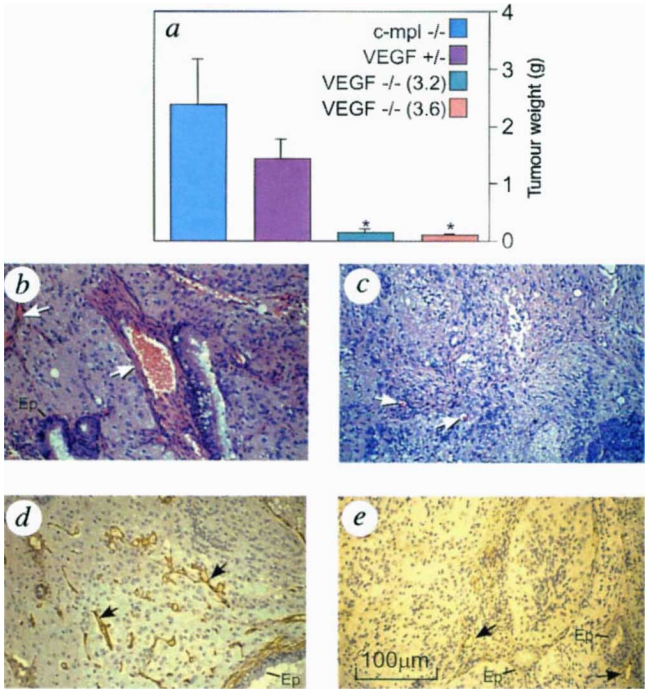

FIG. 2 ES cell tumorigenesis in nude mice. *a*, Tumour weight. *b*, *c*, Haematoxylin and eosin staining and *d*, *e*, immunostaining for CD34 of tumour sections derived from c-*mpl*$^{-/-}$ (*b*, *d*) and *VEGF*$^{-/-}$ (*c*, *e*) ES cells. Histology shows representative sections of teratomas, containing glial tissue, blood vessels (arrowheads) and glandular epithelium (Ep).

METHODS. For injection in nude mice, cells that had been cultured in the presence of leukaemia inhibitory factor were dissociated from stock plates by exposure to 125 mM NaCl, 5 mM KCl, 50 mM HEPES, 5 mM glucose, 1 mM EDTA, pH 7.4; they were washed once, and then resuspended in PBS at the appropriate density. Female Beige nude/xid mice (Charles River, Wilmington, DE) 6–10 weeks old were injected subcutaneously with 1×10^7 cells in the dorsal area in a volume of 0.1 ml ($n = 10$). Values shown in *a* are mean ± s.e.m. of tumour weight determined 4 weeks after cell injection. Statistical analysis was performed by Wilcoxon paired test. Comparison of tumour weight of c-*mpl*$^{-/-}$ group with those of the two *VEGF*$^{-/-}$ clones revealed *P* values < 0.005. The difference in tumour weight between the c-*mpl*$^{-/-}$ and *VEGF*$^{+/-}$ groups was not significant. For immunohistochemistry, a rabbit polyclonal antiserum raised against murine CD34 was used. Primary antibody was detected with streptavidin–biotin by the Vectastain kit, according to the manufacturer's instructions (Vector).

Specific expression of the VEGF mRNA was detected by *in situ* hybridization in both wild-type and heterozygous embryos. Expression of VEGF mRNA in the neuroepithelium is shown in Fig. 4*c*, *d*, *g*, *h*. Thus the *VEGF*$^{+/-}$ phenotype appears to be due to gene dosage and not to maternal imprinting. Although several heterozygous phenotypes have been described[24], this may be the first report that the loss of a single allele of a gene that does not undergo maternal imprinting can be lethal. It is tempting to speculate that, as VEGF concentrations and angiogenic gradients

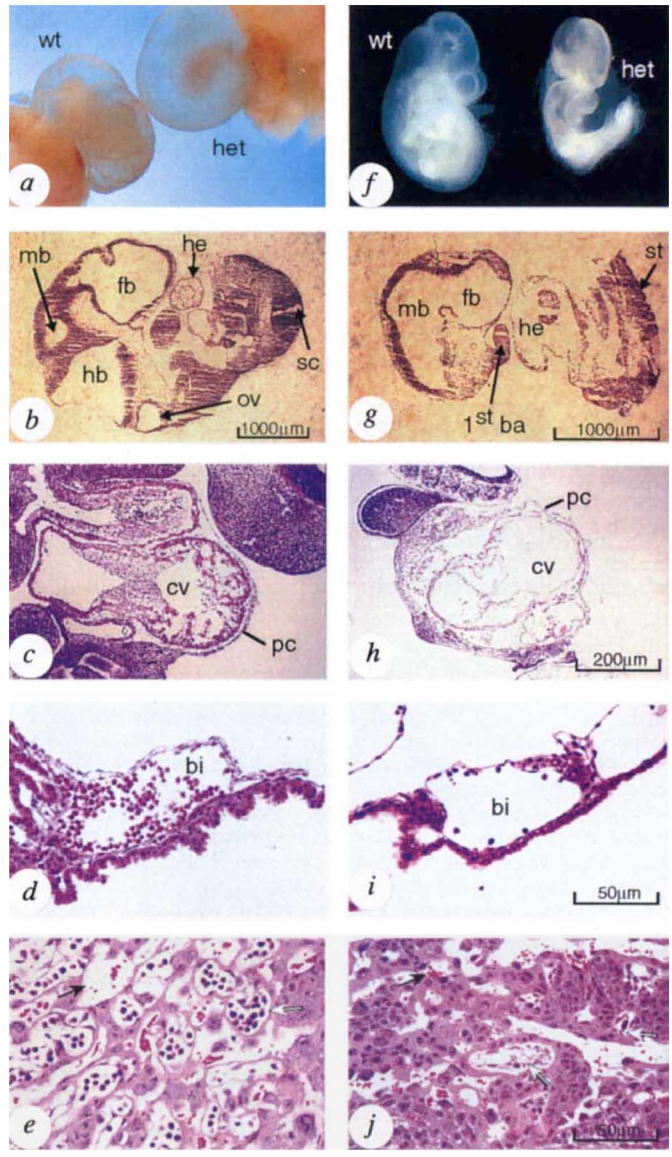

FIG. 3 Gross appearance of wild-type (wt) and heterozygous (het) embryos (*a*, *f*); haematoxylin and eosin stained sections (*b*–*e*, *g*–*j*). All embryos shown are at E10.5. Note the developmental delay and the apparent absence of blood supply in the yolk sac of the heterozygotes. *b*, *g*, Sagittal sections of wt (*b*) and het (*g*) embryos illustrating their development. Sections of wt (*c*) and het (*h*) embryos through the cardiac region demonstrate lack of myoblast differentiation in the heterozygote. *d*, *i*, Yolk sac sections of wt (*d*) and het (*i*) illustrating the scarcity of cellular elements within the blood islands of the het. *e*, *j*, Sections through the placenta. Note the delicate interweaving of maternal (black arrows) and fetal (white arrows) vessels in the wt placenta (*e*), which contrasts with the condensed appearance and presence of degenerating endothelium lining fetal capillaries in the het (*j*). Abbreviations: hb, hindbrain; mb, midbrain; fb, forebrain; ov, otic vesicle; he, heart; sc, spinal cord; st, somites; ba, branchial arch; pc, pericardium; cv, common ventricle; bi (blood islands).

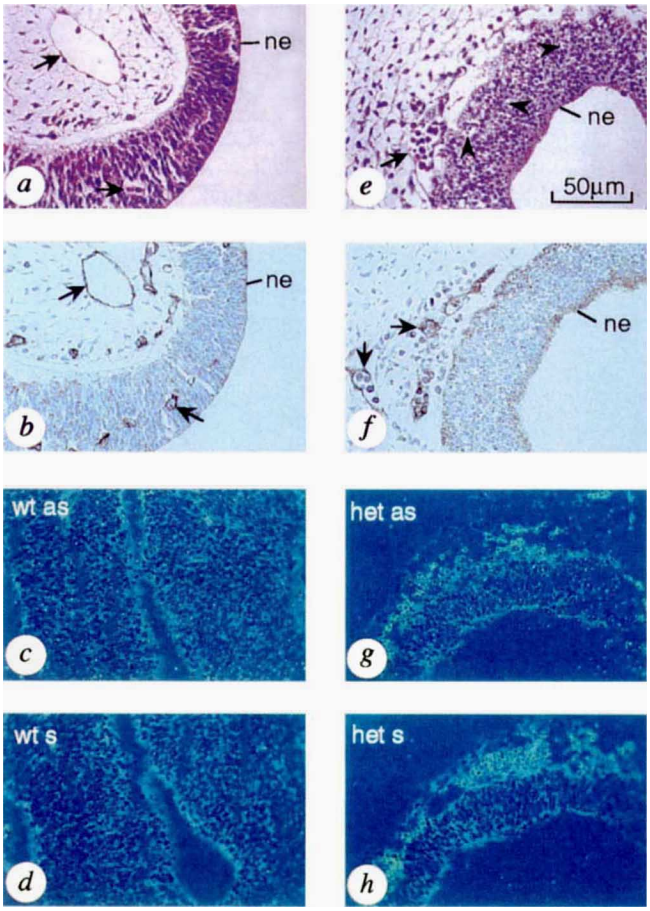

FIG. 4 Haematoxylin and eosin staining (*a*, *e*), CD34 immunostaining (*b*, *f*) and *in situ* hybridization with a probe specific for VEGF (*c*, *d*, *g*, *h*) on sections of neuroepithelium (ne) from wild-type (wt) (*a*–*d*) and heterozygous (het) (*e*–*h*) E10.5 embryos. Arrows indicate blood vessels. Note the absence of blood vessels and the presence of apoptotic cells (arrowheads in *e*) within the neuroepithelium of the het. This contrasts with the well-differentiated and vascularized neuroepithelium in the wt (*a*, *b*). *c*, *d*, *g*, *h*, Hybridization in both wt and het sections incubated with antisense (as) probe but not in those incubates with control sense (s) probe.
METHODS. CD34 immunostaining was performed on tissues that had been fixed in buffered formalin and then paraffin-embedded as described in Fig. 2. For *in situ* hybridization, PCR amplification was used to generate a 251-bp *VEGF* fragment with attached T7 and T3 RNA polymerase promoter sequences to allow RNA production. The *VEGF* probe corresponded to nucleotides 259–509 of the mouse VEGF cDNA[7]. Mouse embryos were fixed in 10% formalin for 2 h and snap-frozen in OCT using hexane, cooled over an acetone/dry ice slurry. Blocks were stored at −80 °C, and ~ 8-μm thick sections were collected on silane-coated slides. Generation of a ^{33}P-UTP labelled antisense and sense RNA hybridization probes and *in situ* hybridization were performed as described[30]. Slides were developed after two weeks.

fall below a threshold during critical periods, this causes irreversible disruption of normal organogenesis. In this context it is noteworthy that thalidomide, which results in severe limb malformations[25] if present even for a short time and at low concentrations in the environment of the early human embryo, has been shown to inhibit angiogenesis[26].

The finding that *VEGF*$^{-/-}$ ES cells are dramatically impaired in their ability to form tumours indicates that, even in a pluripotent system, VEGF is required for effective tumorigenesis and angiogenesis. Finally, although each component of the VEGF/Flt-1/Flk-1 system is required for embryonic development, VEGF is the most critical, as embryonic lethality occurs even in the heterozygous state. □

Received 14 December 1995; accepted 28 February 1996.

1. Folkman, J. & Shing, Y. *J. biol. Chem.* **267,** 10931–10934 (1992).
2. Ferrara, N., Houck, K., Jakeman, L. & Leung, D. W. *Endocr. Rev.* **13,** 18–32 (1992).
3. Dvorak, H. F., Brown, L. F., Detmar, M. & Dvorak, A. M. *Am. J. Path.* **146,** 1029–1039 (1995).
4. Kim, K. J. *et al. Nature* **362,** 841–844 (1993).
5. Adamis, A. P. *et al. Am. J. Ophthalmol.* **118,** 445–450 (1994).
6. Aiello, L. P. *et al. New Engl. J. Med.* **331,** 1480–1487 (1994).
7. Breier, G., Albrecht, U., Sterrer, S. & Risau, W. *Development* **114,** 521–532 (1992).
8. Jakeman, L. B., Armanini, M., Phillips, H. S. & Ferrara, N. *Endocrinology* **133,** 848–859 (1993).
9. Quinn, T., Peters, K. G., deVries, C., Ferrara, N. & Williams, L. T. *Proc. natn. Acad. Sci. U.S.A.* **90,** 7533–7537 (1993).
10. Peters, K. G., deVries, C. & Williams, L. T. *Proc. natn. Acad. Sci. U.S.A.* **90,** 8915–8919 (1993).
11. Fong, G.-H., Rossant, J., Gertenstein, M. & Breitman, M. *Nature* **376,** 66–70 (1995).
12. Shalabi, F. *et al. Nature* **376,** 62–66 (1995).
13. Park, J. E., Chen, H., Winer, J., Houck, K. A. & Ferrara, N. *J. biol. Chem.* **269,** 25646–25654 (1994).
14. Maglione, D., Guerriero, V., Viglietto, G., Delli-Bovi, P. & Persico, M. G. *Proc. natn. Acad. Sci. U.S.A.* **88,** 9267–9271 (1991).
15. Tisher, E. *et al. J. biol. Chem.* **266,** 11947–11954 (1991).
16. Tybulewicz, V. L. J., Crawford, C. E., Jackson, P. K., Bronson, R. T. & Mulligan, R. C. *Cell* **65,** 1153–1163 (1991).
17. Vigon, I. M. *et al. Proc. natn. Acad. Sci. U.S.A.* **89,** 5640–5644 (1992).
18. Risau, W. *et al. Development* **102,** 471–478 (1988).
19. Hilberg, F. & Wagner, E. F. *Oncogene* **7,** 2371–2380 (1992).
20. Pugh, R. B. C. *Pathology of the Testis* (Blackwell, Oxford, 1976).
21. Hogan, B., Beddington, R., Constantini, F. & Lacy, E. *Manipulating the Mouse Embryo* 2nd edn (Cold Spring Harbor Laboratory Press, NY, 1994).
22. Bradley, A. in *Teratocarcinoma and Embryonic Stem Cells: A Practical Approach* (ed. Robertson, E. G.) 113–152 (ERL, Oxford, 1987).
23. Theiler, K. *The House Mouse. Atlas of Embryonic Development* (Springer, New York, 1989).
24. Brandon, E. P., Idzerda, R. L. & McKnight, G. S. *Curr. Biol.* **5,** 625–634 (1995).
25. McBride, W. G. *Lancet* **ii,** 1358–1364 (1987).
26. D'Amato, R. J., Loughnan, M. S., Flynn, E. & Folkman, J. *Proc. natn. Acad. Sci. U.S.A.* **91,** 4082–4085 (1994).
27. Sambrook, J., Fritsch, E. F. & Maniatis, T. *Molecular Cloning, a Laboratory Manual* 2nd edn (Cold Spring Harbor Laboratory Press, NY, 1989).
28. Mansour, S. L., Thomas, K. R. & Capecchi, M. R. *Nature* **336,** 348–352 (1988).
29. Mortensen, R. M., Conner, D. A., Chao, S., Geisterfer-Lowrance, A. A. & Seldman, J. G. *Molec. cell. Biol.* **12,** 2391–2395 (1992).
30. Lu, L. H. & Gillett, N. *Cell Vision* **1,** 169–176 (1994).

ACKNOWLEDGEMENTS. We thank L. Berleau and B. Keyt for radioreceptor assays; P. Young and L. Lasky for *in vitro* experiments on embryoid bodies; J. Park for isolation of cDNA probe; R. Taylor and P. Tobin for histology; A. Ryan for comments and advice; D. Giltinan for statistical analysis; and L. Tamayo and D. Wood for graphics.

CORRESPONDENCE and requests for materials should be addressed to N.F.

Convergence of magno- and parvocellular pathways in layer 4B of macaque primary visual cortex

Atomu Sawatari & Edward M. Callaway

Molecular Neurobiology Laboratory, The Salk Institute for Biological Studies, 10010 North Torrey Pines Road, La Jolla, California 92037, USA

EARLY visual processing is characterized by two independent parallel pathways: the magnocellular stream, which carries information useful for motion analysis, and the parvocellular stream, which carries information useful for analyses of shape and colour[1–3]. Although increasing anatomical and physiological evidence indicates some degree of convergence of the two streams, the pathway through layer 4B of primary visual cortex (V1) and on to higher cortical areas is usually considered to carry only magnocellular input[1–3]. This is inferred from anatomical descriptions of local circuitry in V1, and functional studies of area MT, which receives input from layer 4B[4–7]. We have directly measured the sources of local functional input to individual layer 4B neurons by combining intracellular recording and biocytin labelling with laser-scanning photostimulation[8–10]. We found that most layer 4B neurons receive strong input from both magnocellular-stream-recipient layer 4Cα neurons and parvocellular-stream-recipient layer 4Cβ neurons. Thus higher cortical areas that receive input either directly or indirectly from layer 4B are likely to be more strongly influenced by the parvocellular pathway than previously believed.